

Controlled Emission through Fluorescent Polymer Nanopigments

Dongqing Zhuang and Thio E. Hogen-Esch*

Loker Hydrocarbon Research Institute and Department of Chemistry, University of Southern California, Los Angeles, California 90089-1661

Received March 8, 2010; Revised Manuscript Received July 14, 2010

ABSTRACT: The use is explored of 100–200 nm sized polystyrene or poly(9,9-dihexyl-2,7-fluorenediyl) (PFH) nanoparticles (“nanopigments”) containing low-MW chromophores such as perylene, coumarin 6, and Nile red for use in multicolor emission applications. Good results were obtained with PS nanoparticles at low (≤ 0.5 wt %) chromophore doping levels with emissions being a linear combination of the two component nanoparticles. At higher chromophore concentrations the emissions do not conform to a simple “linear” combination of the component nanoparticles. This may be due to inadvertent dye exchange between nanoparticles during preparation and processing. The emission properties of nanoparticles having blue, green, or red emitting polymer chromophores dispersed in polystyrene or PFH proved more successful in that interparticle dye exchange, and hence undesirable Förster energy transfer, is largely eliminated. Hence, the emissions of these nanopigments are independent and thus can be combined linearly to give a well-controlled emission output.

Introduction

Since the first report on conjugated polymer based light-emitting diodes (pLEDs),¹ significant progress has been achieved in the development of the next generation white and multicolor displays.^{2,3} Organic pLEDs are of special interest due to potential advantages in processing, for instance through spin-casting. Thus far, research on blue emitting polyfluorene based systems have resulted in pLEDs having white displays with external quantum efficiencies being close to that of fluorescent lamps.^{2,3}

A convenient way to produce white emission is to use the complementary color wheel rule using a blue and orange (two-color system)^{3a} or, more commonly, a three-color system (blue, green, and red).^{3b,c} In these cases partial Förster energy transfer between the blue light emitting matrix and chemically bonded or physically dispersed color dopants may be used to produce a white emission. However, the fluorescence typically does not conform to a simple “linear” model and therefore is difficult to program. For instance, for a tricolor system, inadvertent Förster energy transfer, for instance between green and red dyes, makes color tuning difficult (Scheme 1). Hence, an empirical approach is still needed to adjust the composition of the emitting species so that energy transfers result in overall emissions that are located inside the whiteness region defined by the “Commission Internationale de l’Eclairage” (CIE). Although structures consisting of multiple emitting layers are used to cope with these problems, this complicates device engineering.^{4,5}

As shown by Landfester et al., conjugated polymer chromophores can be dispersed in the form of nanoparticles by means of miniemulsions.^{6a–d} Spin-casting or inkjet printing of semiconducting polymers or blends of polymer nanospheres (SPNs) into thin layers has been demonstrated as a new route toward nanostructuring of light-emitting and -harvesting devices.⁶

The pure and controllable color output of core–shell quantum dots (QDs), which differ from that of low MW emitters and conjugated polymers, has long been used in LEDs with or without blending with conjugated polymers.^{7a–d} Recently, Sun et al.

described core–shell quantum dots as emissive layers for the construction of LEDs having four kinds of QDs each emitting a different color.^{7c} Also, Anikeeva et al. reported LEDs with a broad spectral emission generated by electroluminescence from a mixed monolayer of red, green, and blue emitting colloidal QDs in a hybrid organic/inorganic structure.^{7f} For the case of conjugated polymers, Huebner et al. have reported binary color tuning by using colloidal polymer nanoparticle as the primary color sources.^{8a}

Here we demonstrate a first example of the use of polymer-based nanoparticles in linearly tunable fluorescence emissions over a wide range of dye contents using a single wavelength excitation. The nanoparticle sizes determined by dynamic light scattering (Figures S-5 and S-6) are kept between about 100–200 nm⁶ so that interparticle Förster energy transfer should be negligible (Scheme 1).^{8b} Hence, the color output from mixtures of these “nanopigments” should be linear and predictable. Interestingly, very recently Frechet and co-workers reported an analogous example of phosphorescence tuning of cast films by varying the binary composition of two polymer nanoparticle emitters, which were prepared using miniemulsions.^{8c}

In the following we show that this approach is feasible for low-MW chromophores dispersed in PS nanoparticles at low (≤ 0.5 wt %) doping levels. Furthermore, we show that higher doping levels ($> 10\%$) are feasible with polymeric chromophores.

Experimental Section

Materials. Toluene, tetrakis(triphenylphosphine)palladium(0) (Pd(PPh₃)₄, 99%), 9,9-dihexyl-2,7-dibromofluorene (97%), 9,9-dihexylfluorene-2,7-diboronic acid bis(1,3-propanediol) ester (97%), 4,7-dibromobenzo[c]-1,2,5-thiadiazole (95%), 2-(tributylstannyl)thiophene (97%), Aliquat 336, sodium carbonate ($> 99\%$), *N*-bromosuccinimide (99%), perylene ($> 99.5\%$), and coumarin 6 (99+%) were purchased from Aldrich. Sodium dodecyl sulfate (SDS, 97%) and Nile red were purchased from Fluka. One of the polymeric dyes, poly[(9,9-di-*n*-octylfluorenyl-2,7-diyl)-*alt*-(benzo-[2,1,3]thiadiazol-4,8-diyl)] (F8BT, M_n : 5000–8000, $M_w/M_n < 3$), was purchased from Aldrich. All reagents were used as received

*To whom correspondence should be addressed.

Scheme 1. Illustration of a Controlled Color Output by Size Limiting of Nanopigments

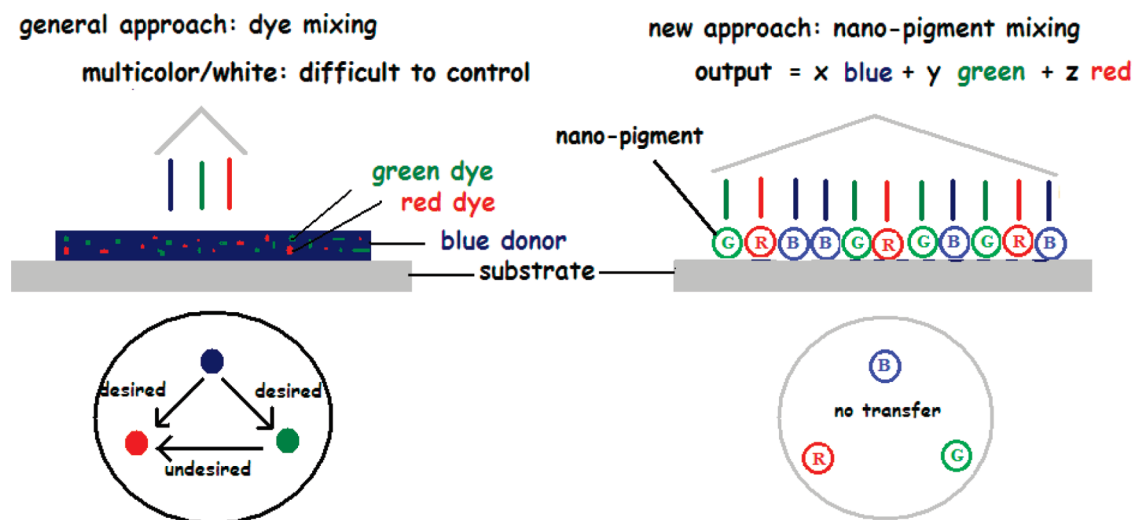


Table 1. Characterization of Low-MW Dye-Doped Nanoparticles

PS/PFH (80/20) ^a nanopigment (emitting color)	dye doping (wt%)	particle size ^b (polydispersity %)	peak emission wavelength (nm)
l-B (blue)	perylene (0.5)	101 (11.9)	425
l-G (green)	coumarin 6 (0.5)	93 (9.2)	574
l-R (red)	Nile red (0.5)	107 (10.6)	423, 484
l-R2 (red)	Nile red (1.0)	72 (6.9)	425, 564

^aWeight ratios. ^bParticle radii in nanometers determined by DLS.

Table 2. Characterization of Nanoparticles for Dicolor and Tricolor Systems

nanopigment ^a (emitting color)	polymer composition ^b	particle size (polydispersity %)	peak emission wavelength (nm)
d-B (blue)	PFH/PS (2/8)	87.2 (11.3)	428
d-G (green)	PFH/F8BT/PS (1/1/8)	106.6 (10.1)	529
t-B (blue)	PFH	64.2 (11.4)	427
t-G (green)	PFH/F8BT (10/1)	43.5 (7.6)	527
t-R (red)	PFH/F6DBT (10/1)	78.0 (12.2)	629

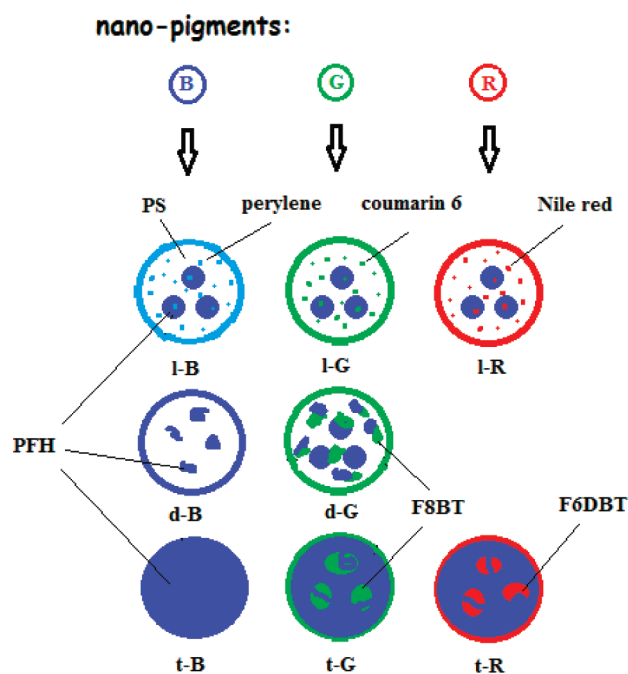
^aThe symbols correspond directly to polymer compositions. ^bWeight ratios.

unless otherwise noted. The polystyrene (PS) was synthesized by ATRP ($M_w = 13\,900$; PDI = 1.10).

Synthesis. The precursor comonomer, 4,7-bis(5-bromo-2-thienyl)-2,1,3-benzothiadiazole, was synthesized as reported.⁹ Proton NMR (250 MHz): δ (CDCl₃) 7.16 (d, ³J: 4 Hz, 2H), 7.80 (s, 2H), 7.81 (d, ³J: 4 Hz, 2H). This comonomer (0.092 g, 0.2 mmol, 10 mol %), 9,9-dihexyl-2,7-dibromofluorene (0.39 g, 0.8 mmol, 40 mol %), and 9,9-dihexylfluorene-2,7-diboronic acid bis(1,3-propanediol) ester (0.5 g, 1.0 mmol, 50 mol %) were copolymerized using the reported Suzuki coupling³ to give 0.48 g of red-emitting polymer poly[(9,9-di-*n*-hexylfluorenyl-2,7-diyl)-*ran*-4,7-bis(2-thienyl)-2,1,3-benzothiadiazole-5,5-diyl] (F6DBT) (yield ~74%). Poly(9,9-dihexyl-2,7-fluorenediyl) (PFH) was also synthesized by Suzuki coupling. The NMR and size exclusion chromatography spectra (SECs) of PFH and F6DBT are shown in Figures S1 and S2.

Preparation of Nanoparticle Emulsions and Films. Following a procedure by Landfester et al.,^{6b} 75 mg of polystyrene (PS) and PFH (PS/PFH, 80/20 wt/wt) and 0.5 wt % of a low-MW chromophore(s) (Table 1) or 10 wt % a polymer dye (Table 2) were dissolved in 3.5 g of chloroform. Into the above solution was added 8 g of aqueous SDS solution (300 mg of SDS in 100 mL of water). The two-phase mixture was emulsified by vigorous stirring (0.5 h) followed by sonication on a Branson S-450D instrument with a flat tip at 90% amplitude for 5 min. The emulsion was then heated with stirring in a 63–65 °C oil bath for 1–2 h to distill off the chloroform, giving 1 wt % aqueous

Scheme 2. Schematic Representation of Nanopigment Used in This Study (for Details See Tables 1 and 2)



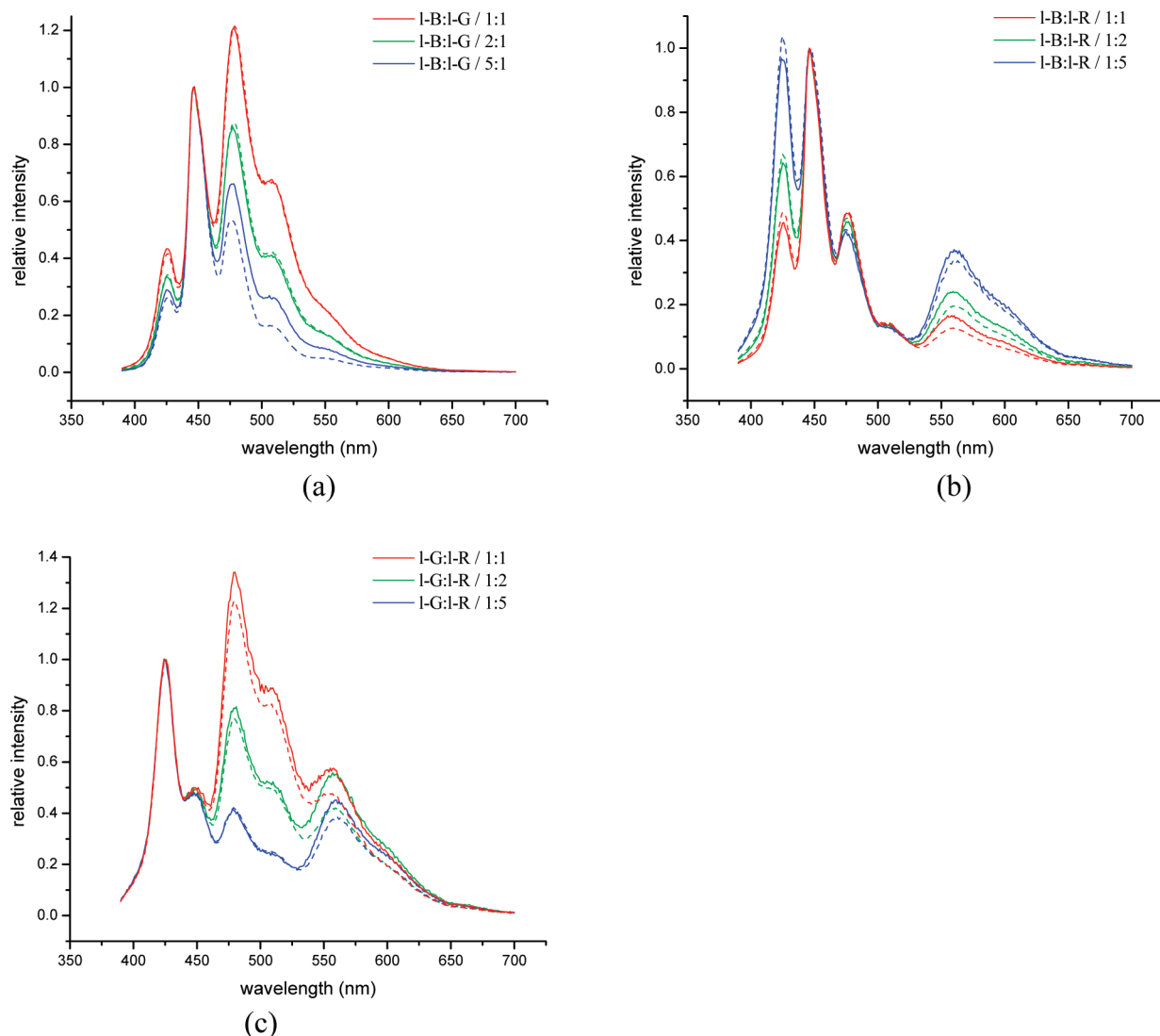


Figure 1. Normalized photoluminescence of films spin-cast from mixture of 1 wt % I-B/I-G (a), I-B/I-R (b), and I-G/I-R PS (c) miniemulsions with different compositions. Solid and dashed lines are experimental and calculated data, respectively. (Normalization coefficients are 1/0.85 for I-B/I-G, 1/0.3 for I-B/I-R, and 1/0.65 for I-G/I-R.)

miniemulsions. These miniemulsions or their mixtures were then spin-cast onto micro cover glasses (VWR, pretreated with a cuvette cleaner) at 6000 rpm for 1 min with Brewer Science Cee-200 coater to give thin films of nanoparticles. The chloroform solutions of polymers and chromophores and their mixtures were also spin-cast into films for comparison.

Characterization. Molecular weights (MWs) of polymers of interest were determined by size exclusion chromatography (SEC) in THF at a flow rate of 1 mL/min (Figure S2) on a Shimadzu Prominence system, equipped with LC-20AT solvent delivery module, RID-10A refractive index detector, Wyatt Dawn light scattering detector, and PLgel 5 μ m MIXED-C column using PS standards. The data were analyzed using LC solution software with GPC option (Figure S2) (PFH MW: M_w = 16 500, PDI = 1.87; F8BT M_w = 16 500, PDI = 2.01; F6DBT: M_w = 18 000, PDI = 1.85). Absorption spectra were recorded on CARY-14 spectrophotometer (Online Instrument Systems). Emission spectra were recorded on a Fluorolog Tau-3 luminescence spectrometer (Jobin Yvon Horiba). Both excitation and emission slit widths were 1 nm. Photoluminescence spectra were recorded by excitation at 365 nm unless noted otherwise. For film samples a front face mode with a 45° angle was used. Particle sizes were measured by dynamic light scattering (DLS) on a Wyatt DynaPro Titan instrument and analyzed by DYNAMICS 6.10 using ten acquisitions per sample.

Results and Discussion

Low-MW Dye-Doped Nanopigments. The control of luminescence of multiple dyes in a single solution deposition process has proved elusive.³ For instance, as shown in Figure S-3, chloroform solutions of PFH/peryene, PFH/coumarin, or PFH/Nile red and their 1/1 mixtures proved unsuitable for control of the desired emissions due to extensive and undesirable Förster transfers between perylene, coumarin, and Nile red.

These problems can be addressed by sol–gel technology for instance in the encapsulation of both low-MW and high-MW chemicals into silica as hybrid materials in applications such as sensors, catalysts, optoelectronic devices, and coatings.¹⁰ Such physical doping is more convenient than chemical bonding of low-MW dyes onto donor materials.

However, dye encapsulation in polymer nanoparticles through the use of miniemulsions (nanopigments) has the potential to avoid energy transfer provided that nanoparticles sizes significantly exceed Förster radii (Scheme 1).^{6c,10} Thus, for spin-cast binary 1:1, 2:1, and 5:1 mixtures of perylene and coumarin 6-doped nanoparticles dispersed in PS/PFH (I-B and I-G) (Scheme 2 and Table 1), the resulting emissions of the 1:1 and 1:2 nanoparticle mixtures were almost indistinguishable from the linear addition of the individual

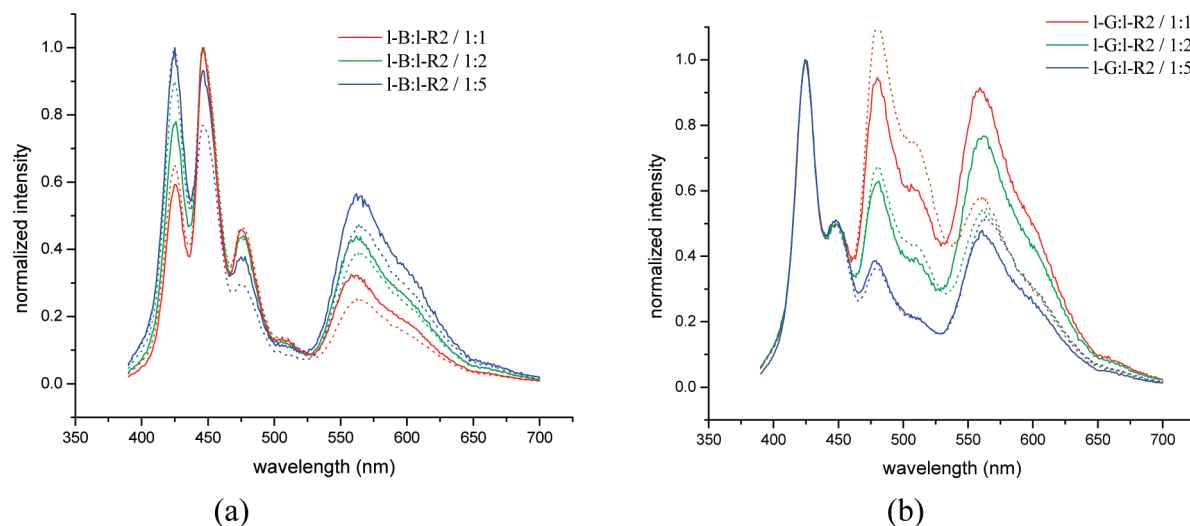


Figure 2. Normalized (450 nm) photoluminescence of films spin-cast from 1 wt % I-B/I-R2 (a) and I-G/I-R2 (b) miniemulsion mixtures with different compositions. Solid and dashed lines are experimental and calculated data, respectively. (Normalization coefficients are 1:0.57 for I-B:I-R2 and 1:0.80 for I-G:I-R2.)

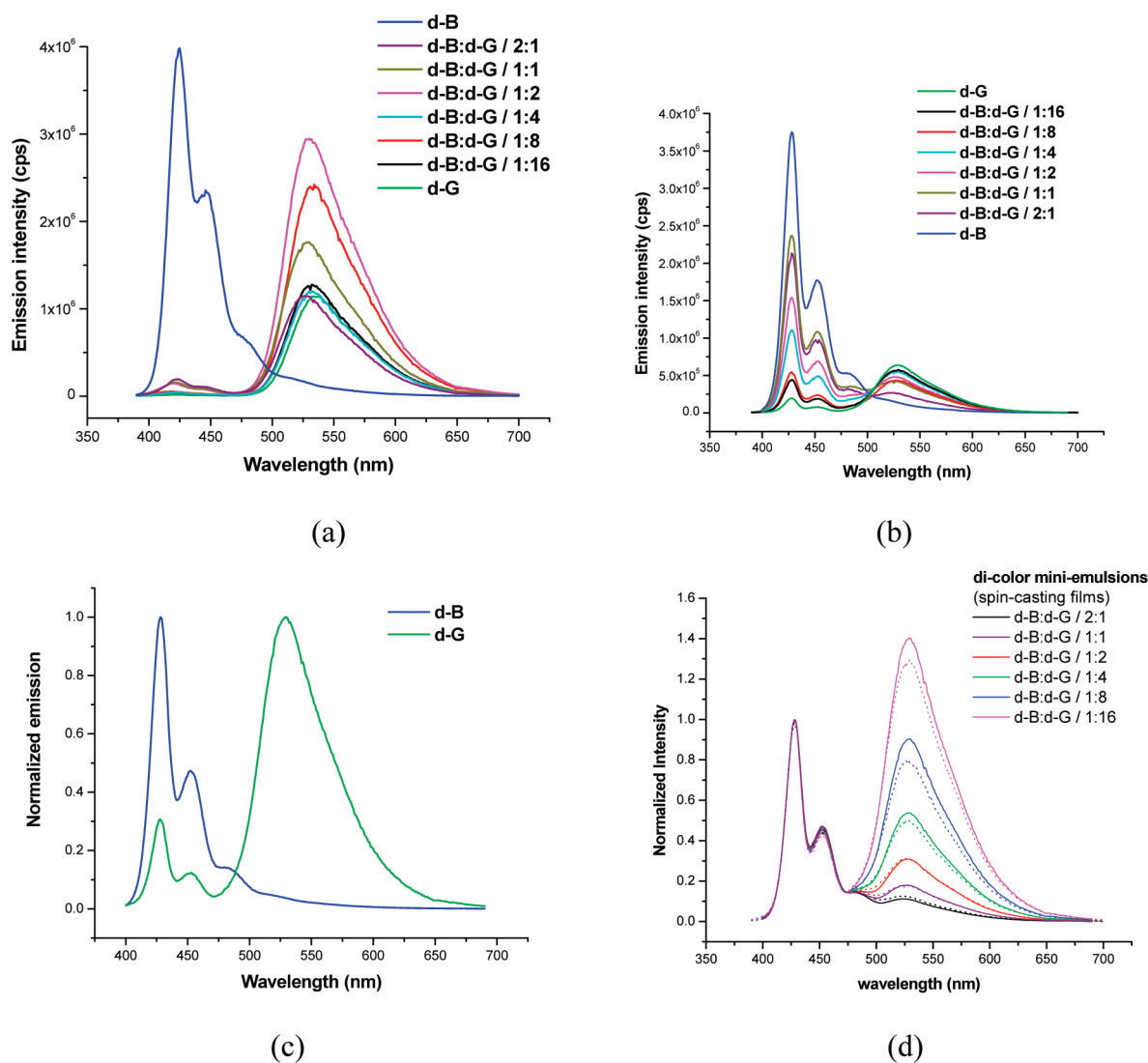
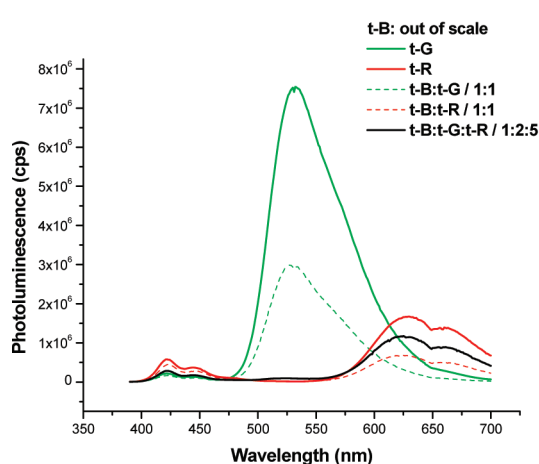
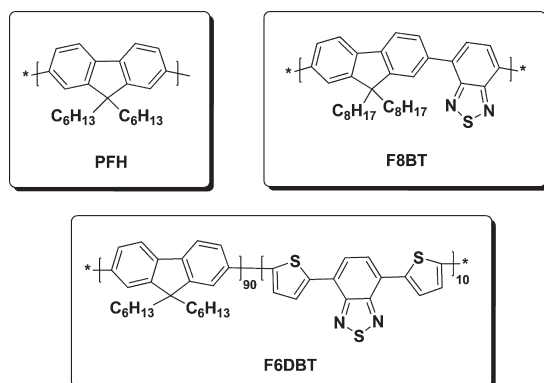


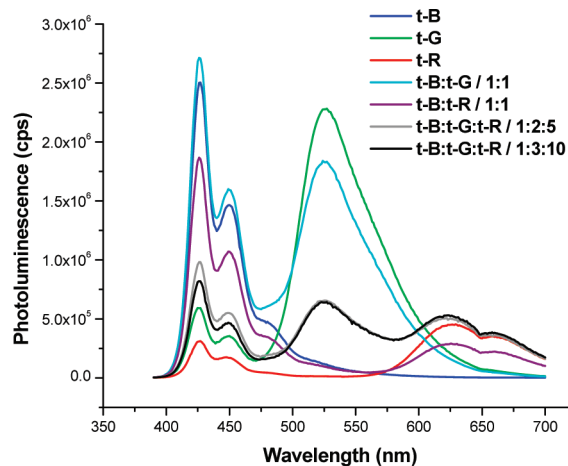
Figure 3. (a) Photoluminescence of films spin-cast from 1 wt % chloroform solutions of d-B, d-G, and their mixtures. (b) Photoluminescence of films spin-cast from 1 wt % d-B, d-G miniemulsions, and their mixtures of a series of compositions. (c) Normalized photoluminescence of d-B and d-G nanoparticle films. (d) Normalized photoluminescence of films spin-cast from 1 wt % d-B/d-G miniemulsion mixtures of a series of d-B/d-G compositions. Solid and dotted lines are experimental and calculated data (normalization coefficient: d-B:d-G/1:0.15), respectively.

nanopigment emissions using single normalization coefficients (Figure 1a).¹¹ For the 5:1 1-B/1-G mixture when normalized at 450 nm, the emission intensities were somewhat greater than calculated at 425 (20%) 475 (25%), and 500 nm (35%). Reasonably good agreement with the calculated spectra was also obtained for the 1-B/1-R and the 1-G/1-R nanoparticle mixtures with emissions being somewhat smaller (5%) at 425 nm and

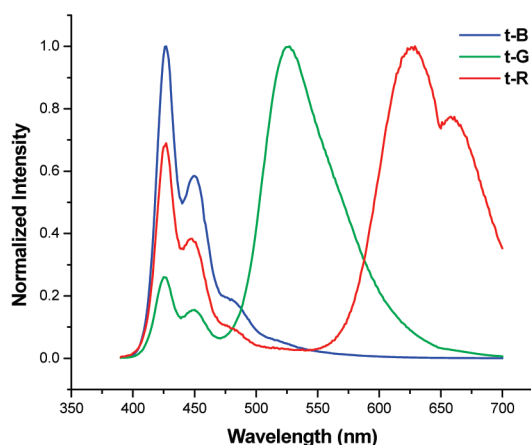
Scheme 3. Structures of Polymer Chromophores



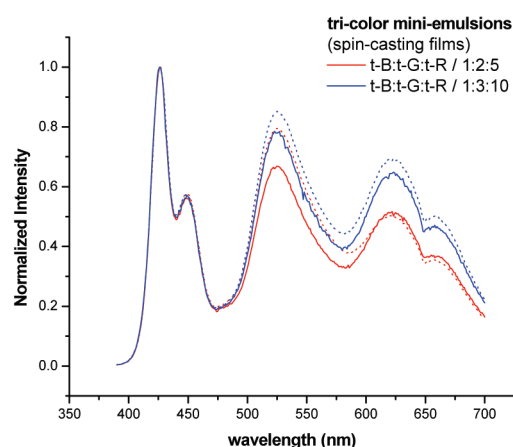
(a)



(b)



(c)



(d)

Figure 4. (a) Photoluminescence of films spin-cast from 1 wt % chloroform solutions of mixtures of t-B, t-G, and t-R. (b) Photoluminescence of films spin-cast from mixtures of 1 wt % t-B, t-G, and t-R miniemulsions. (c) Normalized photoluminescence of t-B, t-G, and t-R nanoparticle films. (d) Normalized photoluminescence of films spin-cast from 1 wt % t-B/t-G/t-R miniemulsion mixtures of different compositions. Solid and dotted lines are experimental and calculated data (normalization coefficient: t-B:t-G/1:0.75; t-B:t-R/1:0.17), respectively.

greater (10–18%) at 575 nm (Figure 1b). Similar small deviations for the 1-G/1-R systems are seen in Figure 1c. In the presence of more Nile red the emissions of the 1-B/R2 or 1-G/R2 nanoparticle films (Table 1 and Figure 2) deviated somewhat more (10–40%) from the calculated linear addition spectra, i.e., for the 1-G/1-R2 mixture (Figure 2b). These effects may be due to inadvertent interfacial Förster transfer consistent with some surface segregation of the dyes in the polymer particles that could have favored interparticle energy transfer. There could also be dye exchange between nanoparticles during solvent evaporation, miniemulsion mixing, or spin-casting.¹²

These results, taken together, indicate potential for physical nanoparticle doping but appear to require further development. Higher dye contents in our hands resulted in extensive interparticle quenching due to surface segregation especially for the relatively hydrophilic Nile red that appears to surface segregate and has a higher partition coefficient compared to coumarin 6 and perylene.¹³

Polymer Chromophore-Doped Nanopigments. Although better results are obtained using the above nanoparticle approach, inadvertent quenching is still a problem. We reasoned that this could be addressed by using polymeric chromophores as the above dye diffusion processes should be eliminated or slowed considerably.¹²

Thus, we selected PFH (blue, d-B and t-B) and blends of PFH/F8BT (green, d-G and t-G) and PFH/F6DBT (red, d-R and t-R) (Scheme 3) as donor and acceptor, respectively (Scheme 2 and Table 2). Their absorption and emission spectra in solution and in the film form are shown in Figure S4. Examples illustrating the emission of the di- and tricolor nanoparticle systems are shown in Figures 3 and 4. Chloroform spin-cast films of the d-B/d-G mixtures (Figure 3a) show dominant energy transfer from PFH to F8BT, resulting in nearly complete green emission even in the presence of the 80 wt % PS matrix. In this case, intraparticle distances between the PFH and F8BT polymers are apparently well within the Förster radii. However, as seen in Figure 3b, when mixed in the form of larger sized (≥ 50 nm) polystyrene based nanoparticles (SPNs) in the form of miniemulsions, the corresponding films of the d-B/d-G nanoparticle mixtures, containing 20 wt % dye dispersed in PS, gave far better agreement with calculated spectra. In this case the nanoparticle color output is not compromised and is nearly identical with the calculated spectra based on simple linear addition as illustrated in Figure 3b,d for six d-B/d-G nanoparticle compositions.

For the ternary t-B/t-G/t-R nanoparticle systems (Table 2), both green-emitting polymer F8BT and red-emitting polymers F6DBT should be good quenchers for the blue-emitting PFH (Figure S4) which is also used as the carrier polymer for the green and red polymer pigments. F6DBT also quenches green emission of F8BT due to good overlap with the absorption band of F6DBT around 540 nm (Figure S4).⁹ Spin-cast films of the three polymer chromophores dissolved in chloroform emit mainly red together with some residual blue consistent with expectations (Figure 4a). However, as shown in Figure 4b,d, the photoluminescence of the corresponding PS based nanoparticle mixtures gives more readily controllable emissions and good agreement with calculated values. Thus, two normalization coefficients for the 1:1 t-B/t-G mixture and the 1:1 t-B/t-R mixture were sufficient to generate the calculated spectra.¹¹ Compared with a 0.5 wt % doping for the case of the low-MW nanopigment dyes, the polymer nanopigments tolerate much higher chromophore fractions (≥ 10 wt %), consistent with lower processing mediated chromophore diffusion rates and other chromophore size related problems.

Intraparticle phase separation has been reported for the nanoparticles prepared from poly(9,9-dioctylfluorene) and F8BT.¹⁴ The PFH/PS nanoparticle has been shown to give phase separation as well,^{14d,e} and presumably this is also the case for the d-G, t-G, and t-R nanoparticles. However, while Förster transfer within each particle may not be homogeneous, such defects are confined within a single nanoparticle, and hence would only decrease "pixel"¹⁵ resolution (~ 100 nm) but not the overall color output. Nevertheless, because of the greater availability and lower costs, it is important to further improve low-MW dye-doped nanoparticle systems. Recently, encapsulation of low MW dyes into polymer nanoparticles by in-situ polymerization has also been developed.¹⁶

In conclusion, we have shown that polymer nanopigments have the potential to provide enhanced control of emission output by using nanopigments containing low-MW and polymeric dyes. Potential applications include nanoparticle mediated multicolor sensing and labeling,^{10d,17} white-light or full-color displays,^{6,7} and automated color matching for fluorescent coatings and inks.^{14b,18}

Acknowledgment. We gratefully acknowledge financial support of this work by Merck KGaA, Darmstadt, Germany. We are grateful to Professor Landfester for providing us with the

protocols used for the nanoparticle preparations. We also thank Victoria Piunova for help with the SEC measurements.

Supporting Information Available: Proton NMR spectra of PFH and F6DBT, SEC spectra of PFH, F8BT, and F6DBT, photoluminescence spectra of small MW dyes and F6DBT, and its absorption spectrum in chloroform. This material is available free of charge via the Internet at <http://pubs.acs.org>.

References and Notes

- (1) Burroughes, J. H.; Bradley, D. D. C.; Brown, A. R.; Marks, R. N.; Mackay, K.; Friend, R. H.; Burns, P. L.; Holmes, A. B. *Nature* **1990**, *347*, 539–541.
- (2) For example: (a) Huang, F.; Shih, P.-I.; Shu, C.-F.; Chi, Y.; Jen, A. K.-Y. *Adv. Mater.* **2009**, *21*, 361–365. (b) Zhen, C.-G.; Chen, Z.-K.; Liu, Q.-D.; Dai, Y.-F.; Shin, R. Y. C.; Chang, S.-Y.; Kieffer, J. *Adv. Mater.* **2009**, *21*, 2425–2429. (c) Wu, H.; Zou, J.; Liu, F.; Wang, L.; Mikhailovsky, A.; Bazan, G. C.; Yang, W.; Cao, Y. *Adv. Mater.* **2008**, *20*, 696–702. (d) Wu, Z.; Xiong, Y.; Zou, J.; Wang, L.; Liu, J.; Chen, Q.; Yang, W.; Peng, J.; Cao, Y. *Adv. Mater.* **2008**, *20*, 2359–64. (e) Pei, Q. *Aldrich Mater. Matters* **2007**, *2* (3), 26–28. (f) Gong, X.; Wang, S.; Moses, D.; Bazan, G. C.; Heeger, A. J. *Adv. Mater.* **2005**, *17*, 2053–2058. (g) Park, J. H.; Lim, Y. T.; Park, O. O.; Kim, J. K.; Yu, J.-W.; Kim, Y. C. *Chem. Mater.* **2004**, *16*, 688–692. (h) Friend, R. H.; Gymer, R. W.; Holmes, A. B.; Burroughes, J. H.; Marks, R. N.; Taliani, C.; Bradley, D. D. C.; Dos Santos, D. A.; Bredas, J. L.; Logdlund, M.; Salaneck, W. R. *Nature* **1999**, *397*, 121–128.
- (3) (a) Liu, J.; Cheng, Y.; Xie, Z.; Geng, Y.; Wang, L.; Jing, X.; Wang, F. *Adv. Mater.* **2008**, *20*, 1357–1362. (b) Liu, J.; Chen, L.; Shao, S.; Xie, Z.; Cheng, Y.; Geng, Y.; Wang, L.; Jing, X.; Wang, F. *Adv. Mater.* **2007**, *19*, 4224–4228. (c) Luo, J.; Li, X.; Hou, Q.; Peng, J.; Yang, W.; Cao, Y. *Adv. Mater.* **2007**, *19*, 1113–1117.
- (4) Kido, J.; Kimura, M.; Nagai, K. *Science* **1995**, *267*, 1332–1334.
- (5) (a) Polikarpov, E.; Thompson, M. E. *Aldrich Mater. Matters* **2007**, *2* (3), 21–23. (b) Sun, Y.; Giebink, N. C.; Kanno, H.; Ma, B.; Thompson, M. E.; Forrest, S. R. *Nature* **2006**, *440*, 908–912. (c) Shen, Z.; Burrows, P. E.; Bulovic, V.; Forrest, S. B.; Thompson, M. E. *Science* **1997**, *276*, 2009–2011.
- (6) (a) Landfester, K. *Adv. Mater.* **2001**, *13*, 765–768. (b) Landfester, K.; Montenegro, R.; Scherf, U.; Guntner, R.; Asawapirom, U.; Patil, S.; Neher, D.; Kietzke, K. *Adv. Mater.* **2002**, *14*, 651–655. (c) Kietzke, T.; Neher, T. D.; Landfester, K.; Montenegro, R.; Gunter, R.; Scherf, U. *Nature Mater.* **2003**, *2*, 408–414. (d) Plok, T.; Gamerith, S.; Gadermaier, C.; Plank, H.; Wenzl, F. P.; Patil, S.; Montenegro, R.; Kietzke, T.; Neher, D.; Scherf, U.; Landfester, K.; List, E. J. W. *Adv. Mater.* **2003**, *15*, 800–804. (e) de Gans, B.-J.; Schubert, U. S. *Langmuir* **2004**, *20*, 7789–7793. (f) Landfester, K. *Top. Curr. Chem.* **2003**, *227*, 75–123.
- (7) (a) Colvin, V. L.; Schlamp, M. C.; Alivisatos, A. P. *Nature* **1994**, *370*, 354–357. (b) Coe, S.; Woo, W.-K.; Bawendi, M.; Bulovic, V. *Nature* **2002**, *420*, 800–803. (c) Li, Y.; Rizzo, A.; Mazzeo, M.; Carbone, L.; Manna, L.; Cingolani, R.; Gigli, G. *J. Appl. Phys.* **2005**, *97*, 113501–113504. (d) Sun, Q.; Subramanyam, G.; Dai, L.; Check, M.; Campbell, A.; Naik, R.; Grote, J.; Wang, Y. *ACS Nano* **2009**, *3*, 737–743. (e) Sun, Q.; Wang, Y. A.; Li, L. S.; Wang, D.; Zhu, T.; Xu, J.; Yang, C.; Li, Y. *Nature Photonics* **2007**, *1*, 717–722. (f) Anikeeva, P. O.; Halpert, J. E.; Bawendi, M. G.; Bulovic, V. *Nano Lett.* **2007**, *7*, 2196–2200.
- (8) (a) Huebner, C. F.; Foulger, S. H. *Langmuir* **2010**, *26*, 2945–2950. (b) Wu, C.; Zheng, Y.; Szymanski, C.; McNeill, J. J. *Phys. Chem. C* **2008**, *112*, 1772–1781. (c) Gao, H.; Poulsen, D. A.; Ma, B.; Unruh, D. A.; Zhao, X.; Millstone, J. F.; Frechet, J. M. J. *Nano Lett.* **2010**, *10*, 1440–1444.
- (9) Hou, Q.; Xu, Y.; Yang, W.; Yuan, M.; Peng, J.; Cao, Y. *J. Mater. Chem.* **2002**, *12*, 2887–2892.
- (10) (a) Coronado, E.; Palomares, E. J. *Mater. Chem.* **2005**, *15*, 3593–3597. (b) Penard, A.-L.; Gacoin, T.; Boilot, J.-P. *Acc. Chem. Res.* **2007**, *40*, 895–902. (c) *Silica-Based Materials for Advanced Chemical Applications*; Pagliaro, M., Ed.; RSC Publishing: London, 2009. (d) Sokolov, I.; Kievsky, Y. Y.; Kaszpurenko, J. M. *Small* **2007**, *3*, 419–423.
- (11) Normalization coefficients are obtained by comparing the emission spectrum of a 1:1 (w/w) mixture of two of the nanoparticles films with the addition of the two nanoparticle film spectra. The normalization coefficient is selected so that the calculated spectrum optimally overlaps with the 1/1 spectrum.

- (12) Wu, M.; Rotureau, E.; Marie, E.; Delacherie, E.; Durand, A. In *Emulsion Science and Technology*; Tadros, T. F., Ed.; Wiley-VCH Verlag: Weinheim, 2009; pp 107–132.
- (13) Based on LogP value from ChemDraw software (Perylene: 5.34; Coumarin6: 5.19; Nile red: 2.98).
- (14) (a) Kietzke, T.; Neher, D.; Kumke, M.; Montenegro, M.; Landfester, K.; Scherf, U. *Macromolecules* **2004**, *37*, 4882–4890. (b) Kietzke, T.; Neher, D.; Kumke, M.; Ghazy, O.; Ziener, U.; Landfester, K. *Small* **2007**, *3*, 1041–1048. (c) Morgado, J.; Moons, E.; Friend, R. H.; Cacialli, F. *Synth. Met.* **2001**, *124*, 63–66. (d) Chappell, J.; Lidzey, D. G. *J. Microsc.* **2003**, *209*, 188–193. (e) Kuo, C. C.; Lin, C. H.; Chen, W. C. *Macromolecules* **2007**, *40*, 6959–6966.
- (15) Random mixtures of SPNs or polymer nanopigments are defined as pixels.
- (16) Steiert, N.; Landfester, K. *Macromol. Mater. Eng.* **2007**, *292*, 1111–1125.
- (17) Han, M.; Gao, X.; Su, J. Z.; Nie, S. *Nature Biotechnol.* **2001**, *19*, 631–635.
- (18) Tsyalkovsky, V.; Klep, V.; Ramaratnam, K.; Lupitskyy, R.; Minko, S.; Luzinov, I. *Chem. Mater.* **2008**, *20*, 317–325.